

RESEARCH ARTICLE

Open Access



Guanine crystal formation by bacteria

María Elisa Pavan¹ , Federico Movilla² , Esteban E. Pavan³ , Florencia Di Salvo² , Nancy I. López^{1,4} and M. Julia Pettinari^{1,4*}

Abstract

Background Guanine crystals are organic biogenic crystals found in many organisms. Due to their exceptionally high refractive index, they contribute to structural color and are responsible for the reflective effect in the skin and visual organs in animals such as fish, reptiles, and spiders. Occurrence of these crystals in animals has been known for many years, and they have also been observed in eukaryotic microorganisms, but not in prokaryotes.

Results In this work, we report the discovery of extracellular crystals formed by bacteria and reveal that they are composed of guanine monohydrate. This composition differs from that of biogenic guanine crystals found in other organisms, mostly composed of β anhydrous guanine. We demonstrate the formation of these crystals by *Aeromonas* and other bacteria and investigate the metabolic traits related to their synthesis. In all cases studied, the presence of the bacterial guanine crystals correlates with the absence of guanine deaminase, which could lead to guanine accumulation providing the substrate for crystal formation.

Conclusions Our finding of the hitherto unknown guanine crystal occurrence in prokaryotes extends the range of organisms that produce these crystals to a new domain of life. Bacteria constitute a novel and more accessible model to study the process of guanine crystal formation and assembly. This discovery opens countless chemical and biological questions, including those about the functional and adaptive significance of their production in these microorganisms. It also paves the road for the development of simple and convenient processes to obtain biogenic guanine crystals for diverse applications.

Keywords Biogenic guanine crystals, Guanine monohydrate, Melanin, *Aeromonas*, Biomaterial, Bacterial guanine crystals

Background

Guanine is a purine, one of the four bases of the nucleotides that constitute the backbone of nucleic acids. Guanine crystals have been observed in diverse organisms [1–3]. The most widely studied are related to the production of structural color or are part of the reflective tissue in visual organs in many animals, including arthropods, mollusks, amphibians, reptiles, and fish [2]. The extensive occurrence of guanine crystals in optical systems is probably due to its exceptionally high refractive index and to the fact that guanine is a widespread and abundant metabolite [4]. Guanine can also be excreted as an end product of nitrogen metabolism. Guanine crystals have long been known to be among the main excretion products in arachnids [5] and more recently found in land

*Correspondence:

M. Julia Pettinari
jul@qb.fcen.uba.ar

¹ Departamento de Química Biológica, Facultad de Ciencias Exactas y Naturales, Universidad de Buenos Aires, Buenos Aires, Argentina

² Departamento de Química Inorgánica, Analítica y Química Física e INQUIMAE-CONICET, Facultad de Ciencias Exactas y Naturales, Universidad de Buenos Aires, Buenos Aires, Argentina

³ Biomedical Technologies Laboratory, Department of Electronics, Information and Bioengineering, Politecnico Di Milano, Milan, Italy

⁴ IQUBICEN-CONICET, Facultad de Ciencias Exactas y Naturales, Universidad de Buenos Aires, Buenos Aires, Argentina



© The Author(s) 2023. **Open Access** This article is licensed under a Creative Commons Attribution 4.0 International License, which permits use, sharing, adaptation, distribution and reproduction in any medium or format, as long as you give appropriate credit to the original author(s) and the source, provide a link to the Creative Commons licence, and indicate if changes were made. The images or other third party material in this article are included in the article's Creative Commons licence, unless indicated otherwise in a credit line to the material. If material is not included in the article's Creative Commons licence and your intended use is not permitted by statutory regulation or exceeds the permitted use, you will need to obtain permission directly from the copyright holder. To view a copy of this licence, visit <http://creativecommons.org/licenses/by/4.0/>. The Creative Commons Public Domain Dedication waiver (<http://creativecommons.org/publicdomain/zero/1.0/>) applies to the data made available in this article, unless otherwise stated in a credit line to the data.

crustaceans [6]. In eukaryotic microorganisms, guanine crystal-like particles were observed in the cytoplasm of paramecia and other protozoa [7] and in several microalgae [8] such as dinoflagellates [9]. Guanine crystals in these organisms have been proposed to act as purine storage reservoirs, and used as a source of purines and organic nitrogen during starvation [7, 8].

There are three crystal forms for guanine, two polymorphs of the anhydrous phases, the α and β forms [10, 11], and the monohydrate [12]. The three forms have been obtained *in vitro*, displaying different morphologies: the α and β polymorphs showed a prismatic bulky morphology, while guanine monohydrate formed elongated needle-like crystals [13]. Biogenic guanine crystals are typically composed of anhydrous guanine and studies that have analyzed its crystalline form (obtained from spiders, fish, and copepods) confirmed the presence of the β polymorph in all cases [13].

While guanine crystals have been observed in diverse groups of animals and in eukaryotic microorganisms, these biogenic crystals have not been reported in prokaryotes. Analysis of bright crystals observed in colonies of melanogenic *Aeromonas salmonicida* subsp. *pectinolytica* 34mel^T [14] revealed that the crystals are composed of guanine monohydrate, very rarely found in nature. Careful examination allowed the discovery of guanine monohydrate crystals in other bacteria as well. This work describes the characteristics of bacterial guanine crystals and investigates the metabolic traits that could lead to the synthesis of these crystals in bacteria.

Results and discussion

Crystals found in bacterial colonies

Serendipitous observation of month-old colonies of the melanogenic bacterium *A. salmonicida* subsp. *pectinolytica* strain 34mel^T (from now on, 34mel) revealed the presence of glimmering crystals in contrast with the dark background. These particles were associated to the colonies and not the surrounding medium and appeared as birefringent crystalline material under polarized light (Additional file 1: Fig. S1). Scanning electron microscopy (SEM) showed that the crystalline material consisted of mesoscopically structured 50 to 100 μm sphere-like aggregates of elongated nanocrystals (Fig. 1A–C). The crystals were also observed when 34mel was cultured in liquid medium (Fig. 1D–F). Organization of biogenic crystals in complex mesoscopic structures such as the skeletal structures composed of calcium carbonate found in sea urchin spines and mollusk nacre have been extensively studied [15]. Organic biogenic crystals such as those composed of guanine often have special arrangements that can enhance their properties [16–18]. Guanine crystals found in animals are normally described as platelets or prisms that can be arranged in blocks and are often found in specific layered tissues [1, 2, 19]. In eukaryotic microorganisms, packed prismatic particles of guanine crystals have been observed inside intracellular vesicles [3, 20]. The rounded aggregates of nanocrystals produced by the bacteria are very different from the structures observed in other biogenic crystals.

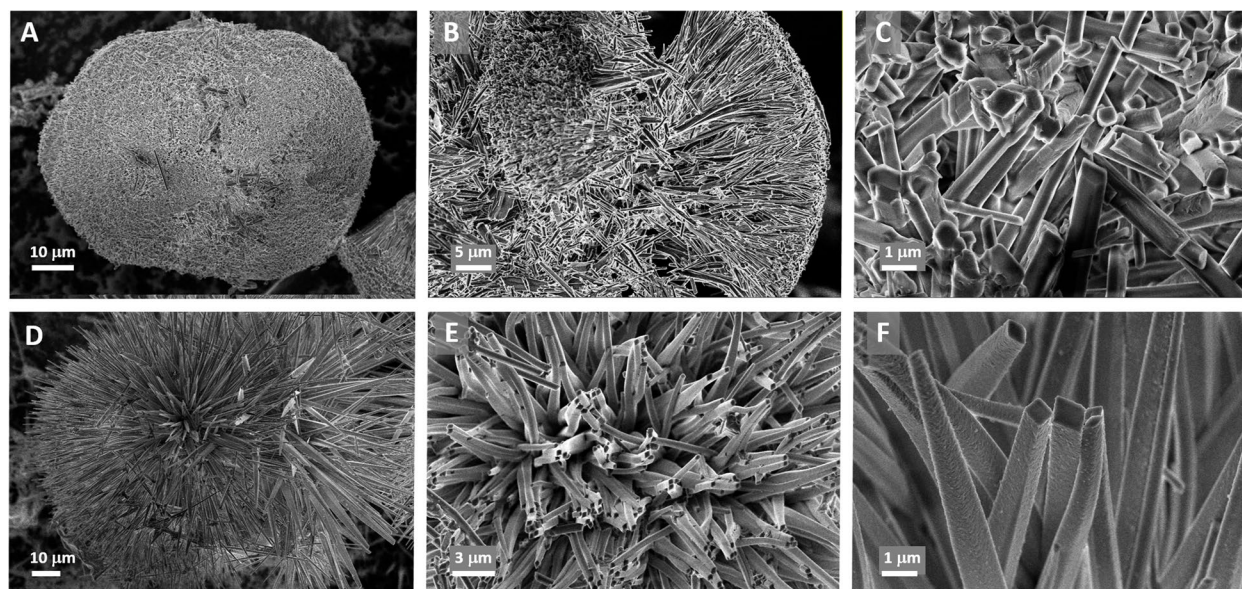


Fig. 1 SEM micrographs of the crystalline material produced by 34mel. Crystalline aggregates and individual nanocrystals found in bacterial cultures grown in solid (A–C) and liquid (D–F) LB medium (increasing levels of magnification from left to right)

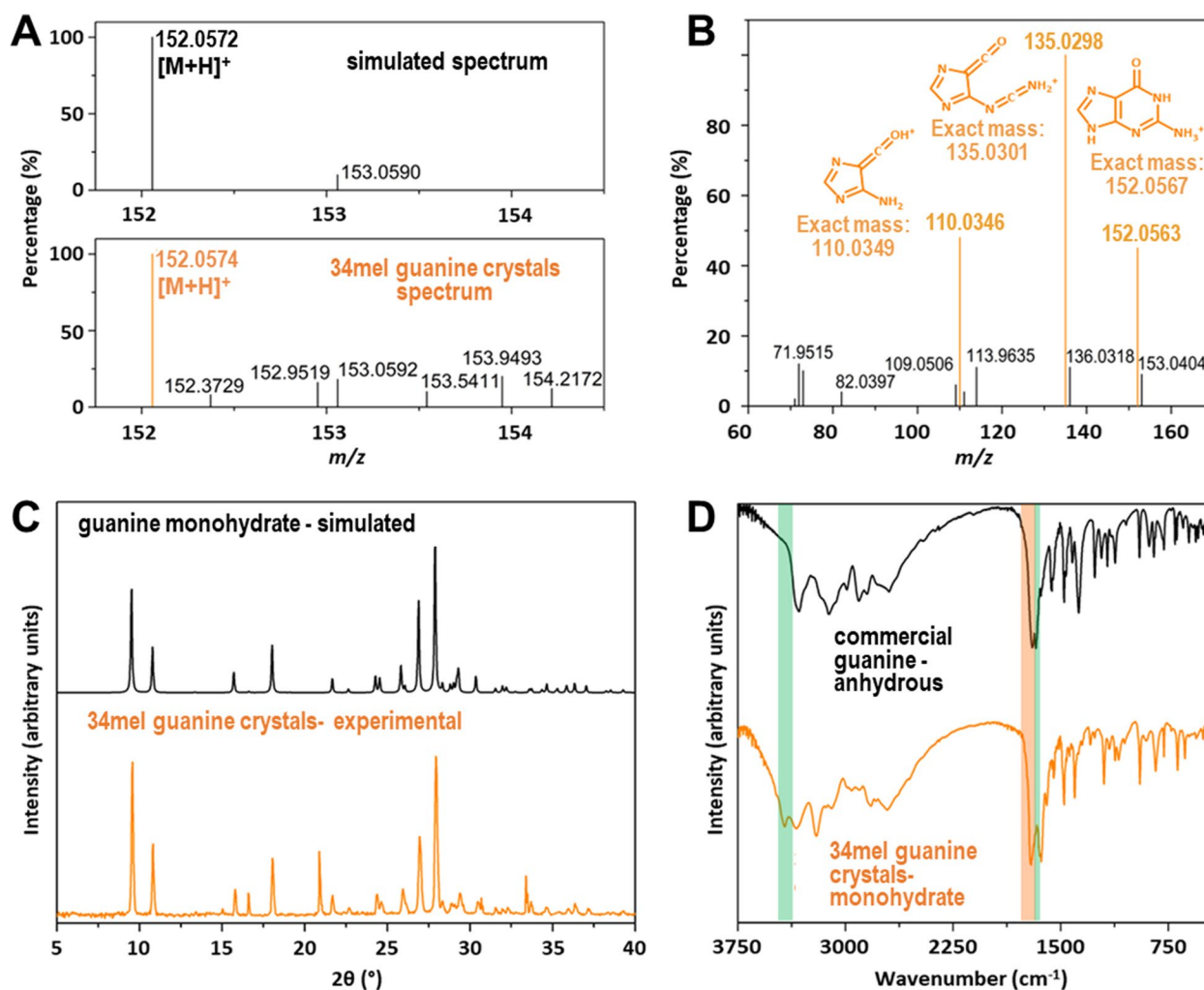


Fig. 2 Characterization of guanine monohydrate crystals produced by 34mel. **A** ESI-MS spectrum of biogenic guanine compared to the simulated data for guanine. **B** ESI MS/MS spectrum of the $[M+H]^+$ ion m/z 152.0574. Solvent: methanol; H_2O . In color, proposed structures for MS/MS obtained ions are shown. **C** Powder X-ray diffraction pattern of the biogenic guanine crystals and the simulated powder X-ray diffraction pattern obtained from the guanine monohydrate single-crystal X-ray data [12]. **D** FT-IR spectra of biogenic crystals and commercial guanine, signals associated with water molecules are highlighted in green and those of carbonyl and amine groups in orange

The morphology of the nanocrystals found in 34mel cultures can be described predominantly as rhomboidal or hexagonal elongated prisms, with an average size of the base around $500 \text{ nm} \times 350 \text{ nm}$ and a maximum length of about $10 \mu\text{m}$ (Fig. 1 and Additional file 1: Fig. S2). The size of the base of the nanocrystals is comparable to prismatic biogenic guanine crystals observed in some spiders [19], but the bacterial crystals are considerably more elongated (Fig. 1).

Characterization of the crystalline material

The structural analysis of the crystals produced by 34mel was performed on bulky samples obtained after collection, washing and drying under vacuum, using different

spectroscopy and X-ray diffraction studies (XRD) and CHN elemental analysis. High-resolution electrospray ionization mass spectrometry (HR ESI-MS) of the crystals showed a signal at m/z 152.0574 corresponding to the ion $[M+H]^+$ (Fig. 2A and Additional file 2: Fig. S3). MS/MS experiments for the target ion gave place to the expected fragments for guanine [21] (Fig. 2B). The assignment was confirmed by comparison with commercial guanine run under the same experimental conditions (Additional file 2: Fig. S4). The aggregation of guanine in solution is clearly demonstrated by the presence of ions with $m/z > 152$ associated to $[nM+H]^+$ and $[nM+Na]^+$ mainly (Additional file 2: Fig. S3). ^1H NMR (Additional file 2: Fig. S5), FT-IR (Fig. 2D), UV-visible (Additional file 2: Fig. S6) spectroscopy, and

XRD (Fig. 2C and Additional file 3: Fig. S7) results confirmed that the crystalline material corresponded to guanine crystals.

Although these characterization techniques allowed us to determine that guanine was the major component in all the crystalline samples, only solid state characterization studies gave information regarding the crystalline form of the guanine produced by 34mel. Powder X-ray diffraction patterns of bacterial crystal samples showed a very good fit with the data reported for the monohydrate phase, one of the three crystal forms of guanine known to date [10–12] (Fig. 2C and Additional file 3: Fig. S7). In the FT-IR spectrum, the signals at 3425 and 3200 cm^{-1} , and the one at 1590 cm^{-1} , associated to the stretching modes ν_1 and ν_3 , and the bending mode ν_2 of water molecules, respectively (Fig. 2D). The carbonyl and primary amine stretching modes that generate two resolved signals at 1681 cm^{-1} and 1632 cm^{-1} are also in agreement with previously reported data for the guanine monohydrate crystalline phase [13]. Elemental analysis revealed a high N content compound (C 35.2%, H 4.2%, N 37.1%), similar to the calculated composition for a sample of guanine monohydrate containing traces of melanin and water (please refer to Additional file 2 for details).

The crystal structure of guanine monohydrate was determined in 1971 [12], and only a few years ago, a detailed study of guanine crystallization in solution provided experimental data of this phase [13]. As described, the crystals found in 34mel are elongated prisms (Fig. 1B, C, E, F), a crystalline habit resembling the one obtained for the guanine monohydrate *in vitro* [13], and different from the crystals formed by anhydrous guanine [2].

Guanine monohydrate crystals produced by 34mel are brown even after several steps of purification with different solvents. This coloring could be associated with the homogentisate melanin synthesized by the microorganism if traces of the pigment were included in the crystalline structure of the guanine. Crystallization experiments of commercial guanine were performed in basic and acidic conditions *in vitro*, including melanin (obtained from the bacteria) in the solution, and the crystalline material obtained was analyzed through powder XRD (please refer to Additional file 3 for details). For every condition tested, the addition of melanin resulted in brown crystals, but the same crystalline phase was observed for the samples with or without biogenic melanin (Additional file 3: Figs. S8, S9). Furthermore, guaninium chloride dihydrate crystalline material obtained from acidic solutions containing biogenic melanin was suitable for single crystal XRD structural determination. Crystallographic data did not show any dye molecules in the structure (Additional file 3: Fig. S10 and Table S1). These results confirmed that the color providing substance

(melanin) did not alter the crystal packing and structural parameters (Additional file 3: Table S2), in agreement with a recent study where it is shown that intracrystalline dopants do not alter the morphology of biogenic guanine crystals [19].

Biological and genetic aspects of guanine crystal synthesis in bacteria

Guanine crystals are found in many animals in specialized cells such as guanocytes in spiders [22] or iridophores in fish [23]. In eukaryotic microorganisms including many microalgae, intracellular guanine crystals are found in vacuoles [3, 20]. The formation of intracellular crystals in bacteria has been reported in very few cases, such as the membrane-surrounded magnetite crystals in magnetotactic bacteria [24] or the parasporal crystals formed by the Cry protein in *Bacillus thuringiensis* [25]. The bacterial guanine crystals observed in this study are extracellular, with a size that is several times larger than the cells, and structured in large crystalline aggregates, differing both in location and morphology when compared to biogenic guanine crystals formed by other organisms.

In nature, purines are synthesized as nucleotides in the so-called *de novo* pathway. Enzymatic removal of the phosphate and sugar from the nucleotides yields the corresponding bases. Nucleosides and free bases released from nucleic acid breakdown are recycled through the salvage pathway or degraded to uric acid. Guanine accumulation leading to crystal formation in animals has been related to upregulation of the guanine portion of the *de novo* purine synthesis [26] or attributed to deficiencies in enzymes involved in guanine degradation, such as xanthine dehydrogenase [5] or guanine deaminase [27, 28].

Purine metabolic pathways were analyzed in 34mel, all other sequenced *Aeromonas* species and some related bacteria. Special emphasis was placed on guanine degradation and the purine nucleotide salvage pathway (Fig. 3A).

Interestingly, the gene coding for the guanine deaminase, commonly present in prokaryotes [30], is absent in 34mel. The lack of this enzyme would prevent the degradation of guanine that could only be recycled back to the nucleoside monophosphate through the salvage pathway (Fig. 3A), potentially leading to guanine excess that would be available for crystal formation. A comparative genomic search in all *Aeromonas* revealed that the genes coding for the guanine deaminase and the three xanthine dehydrogenase subunits are clustered in some species such as *A. hydrophila*. However, this gene cluster is absent in 34mel (Fig. 3B) and in about half of the genomes, and a deeper analysis revealed the occurrence of deletions that affect this region, involving different phylogenetic clades

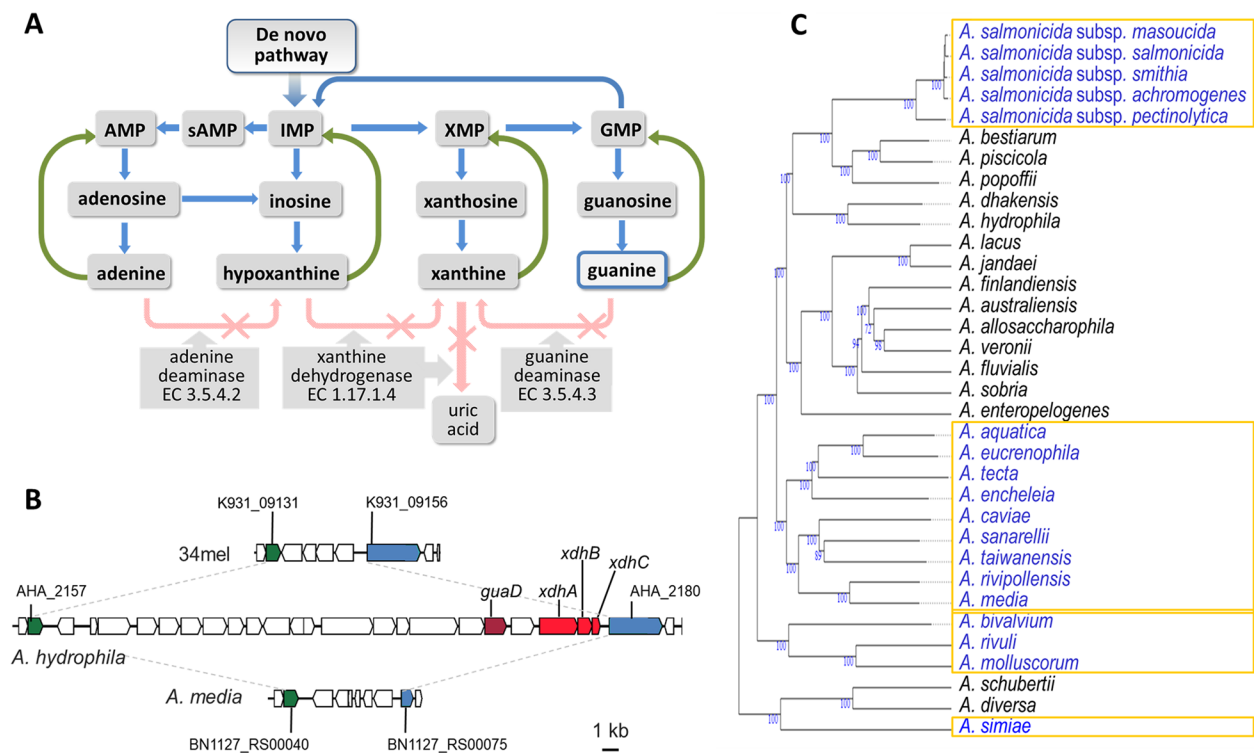


Fig. 3 Purine metabolism in *Aeromonas*. **A** Purine metabolic pathway in 34mel, showing *de novo* formation of purines (blue arrows) and salvage reactions (green arrows). Enzymes absent in 34mel with the corresponding E.C. numbers are shown with crossed out arrows. **B** Comparison of the genomic region containing *guaD* and *xdhABC* in *A. hydrophila* showing their absence in representative *Aeromonas*. Homologous flanking genes are shown: auxin efflux carrier family transporter (green) and ExeM/NucH family extracellular endonuclease (blue) along with the locus tags in each genome. **C** Phylogenomic tree of *Aeromonas* species showing the presence (black) or the absence (blue) of the gene encoding the guanine deaminase. The numbers below branches are GBDP pseudo-bootstrap support values > 60% from 100 replications, with an average branch support of 94.4%. The tree was rooted at the midpoint [29]. The strains used and the accession numbers of their genomes are indicated in Additional file 4: Table S3

(Fig. 3C). Alterations in the salvage pathway can also lead to guanine accumulation. For example, an *Escherichia coli* strain (NR17793) accumulates guanine due to a mutation in *gpt*, the gene encoding guanine phosphoribosyltransferase that catalyzes the conversion of guanine to GMP in the guanine salvage pathway [31]. This *E. coli* strain was grown in LB to analyze if guanine accumulation led to the formation of crystals, but none were observed after more than 30 days, suggesting that guanine accumulation alone is not enough to allow crystal formation and that this process probably involves several factors.

Since 34mel lacks the guanine deaminase and produces melanin, the occurrence of crystals was investigated in strains of *Aeromonas* with different combinations of these traits to analyze the possible relationship of melanin synthesis with guanine crystal formation (Fig. 4). Guanine crystals were observed in melanogenic *A. media* (Fig. 5 and Additional file 1: Fig. S2) and *A. salmonicida* subsp. *salmonicida* but also in the non-melanogenic *A. salmonicida* subsp. *masoucida* (Fig. 5) and *A. caviae*. All these guanine crystal forming bacteria are devoid

of guanine deaminase (Fig. 4). In contrast, no crystals were produced by *A. hydrophila* that carries the guanine deaminase. Careful observation of cultures of field strains of *A. allosaccharophila*, *A. bestiarum*, and *A. veronii* [32] showed that they were also devoid of guanine crystals. Although there is no available genomic sequence information for the strains used, analysis of the genomes of sequenced type strains of these species has revealed the presence of the genes coding for the guanine deaminase (Fig. 4).

When cultures of other bacteria were searched for guanine crystals it was observed that *E. coli* and several species of *Pseudomonas* did not produce them and analysis of their genomes revealed that they carry the guanine deaminase gene (Fig. 4). Instead, guanine crystals were found in *Shewanella oneidensis*, a melanin producing bacterium that lacks the guanine deaminase gene (as observed in crystal producing *Aeromonas*) (Fig. 4). Crystals formed in melanogenic *A. media* and *S. oneidensis* and in non-melanogenic *A. salmonicida* subsp. *masoucida* observed through SEM (Fig. 5A–C) have different

	genes		phenotype	
	<i>guaD</i>	<i>xdh</i>	melanin	crystals
<i>A. salmonicida</i> subsp. <i>pectinolytica</i> 34mel ^T	no	no	●	◇
<i>A. salmonicida</i> subsp. <i>salmonicida</i> ATCC 33658 ^T	no	no	●	◇
<i>A. salmonicida</i> subsp. <i>masoucida</i> NBRC 13784 ^T	no	no	-	◇
<i>A. media</i> CECT 4232 ^T	no	no	●	◇
<i>A. hydrophila</i> ATCC 7966 ^T	yes	yes	-	-
<i>A. caviae</i> C	no*	no*	-	◇
<i>A. allosaccharophila</i> A1	yes*	yes*	-	-
<i>A. bestiarum</i> B1	yes*	yes*	-	-
<i>A. veronii</i> V1	yes*	yes*	-	-
<i>S. oneidensis</i> MR-1 ^T	no	no	●	◇
<i>E. coli</i> K-12 substr. BW25113	yes	yes	-	-
<i>P. aeruginosa</i> PAO1	yes	yes	-	-
<i>P. extremaustralis</i> DSM 25547	yes	yes	-	-
<i>P. protegens</i> Pf-5	yes	yes	-	-
<i>P. putida</i> KT2440	yes	yes	-	-
<i>P. syringae</i> B728a	yes	yes	-	-

Fig. 4 Experimental analysis of guanine crystal formation and melanin production in selected bacterial species. Comparative information related to the presence of genes encoding guanine deaminase (*guaD*) and xanthine dehydrogenase (*xdh*) is included. The symbol * indicates that the genome for the corresponding strain is not available, but the gene(s) is (are) present or absent in the type strain of the species (genome information in Additional file 4: Table S3). Presence of melanin and/or guanine crystals is indicated by colored circles or diamonds

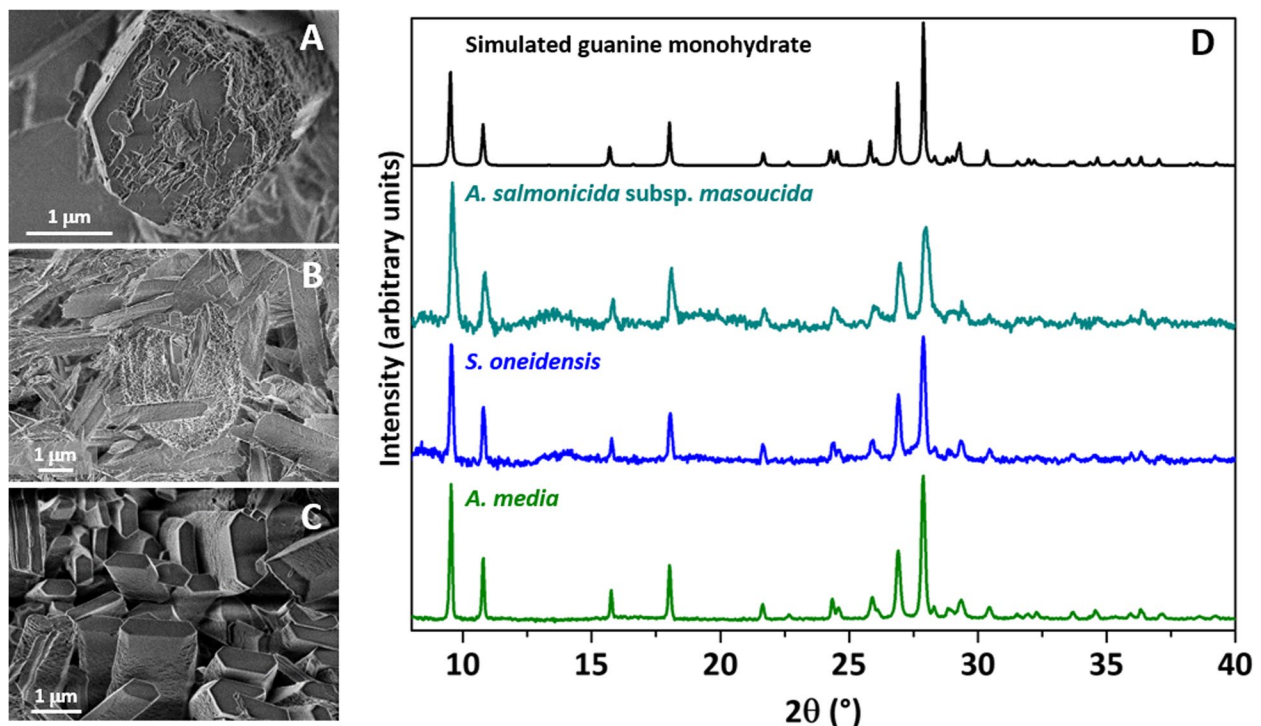


Fig. 5 Characterization of guanine monohydrate crystals produced by several bacteria. **A–C** SEM micrographs of the crystals produced by the bacteria *A. salmonicida* subsp. *masoucida* (**A**), *S. oneidensis* (**B**), and *A. media* (**C**). **D** Powder X-ray diffraction patterns of the crystals produced by the different bacteria and the simulated powder X-ray diffraction pattern obtained from the guanine monohydrate single-crystal X-ray data [12]

sizes but share a prismatic crystal morphology. Powder XRD studies revealed that the diffraction patterns of the crystalline material found in these bacteria have a very good agreement with the calculated data for the guanine monohydrate crystal form (Fig. 5D). These results suggest that this composition could be characteristic of bacterial guanine crystals, differing from the composition commonly found in eukaryotes. All reports of guanine crystals in animals have described them as composed of anhydrous guanine [11]. In the case of eukaryotic microorganisms, although purine crystals have been known for many years, their composition has been investigated in detail in the last years [3]. In a very recent study that investigated crystalline inclusions in diverse unicellular eukaryotes, almost all guanine crystals contained anhydrous guanine with just a few examples containing the monohydrate form [33]. It is possible that detailed analysis of other bacteria could lead in the future to the discovery of other kinds of organic crystals, as already observed in eukaryotes [33].

Guanine crystals are associated with melanin in many organisms [2, 34, 35]. In bacteria that produce homogentisate melanin such as 34mel, melanin synthesis can be inhibited by the herbicide bicyclopiron [36]. When 34mel was grown in the presence of this inhibitor, crystals with similar morphology were observed, although formation was delayed by several days (Additional file 1: Fig. S2). The occurrence of guanine monohydrate crystals in non-melanogenic bacteria, together with the observation of crystals in 34mel in the presence of the inhibitor, indicate that melanin synthesis is not essential for guanine crystal formation.

The results presented in this work show that the presence of the crystals in bacteria correlated with the absence of guanine deaminase, which could lead to guanine accumulation providing the substrate for crystal formation. Furthermore, a phylogenetic analysis of the occurrence of deletions involving the gene coding for this enzyme within the genus *Aeromonas* revealed that its loss seems to be the result of several independent events (Fig. 3C). When guanine crystal production was studied in animals, a patchy phylogenetic distribution was observed [2], suggesting that both in bacteria and in animals, guanine crystal formation arose several times independently.

Conclusions

The existence of guanine crystals in several groups of animals has been known for many years, and their contribution to structural color and as part of reflective tissues has been extensively studied [2, 37]. Their occurrence in other organisms, such as unicellular

eukaryotes, was reported many years ago [9, 38] and thought to be limited to a few cases. Recent renewed interest in guanine crystals and the application of new technologies have expanded this knowledge, and a very recent study showed them to be widespread among eukaryotic microorganisms [33]. Our work has demonstrated their presence in prokaryotes, extending the range of guanine crystal producing organisms to a new domain of life. Future studies will indicate if this capability is restricted to a few bacteria or is more extended among the prokaryotes. The finding of the hitherto unknown guanine crystal formation in prokaryotes has opened countless chemical and biological questions, including those about the functional and adaptive significance of their production in these microorganisms.

Methods

Bacterial strains and culture conditions

A. salmonicida subsp. *pectinolytica* 34mel^T (DSM 12609^T), *A. salmonicida* subsp. *masoucida* NBRC 13784^T, *A. media* CECT 4232^T, *A. hydrophila* ATCC 7966^T and field strains *A. caviae* C, *A. allosaccharophila* A1, *A. bestiarum* B1, and *A. veronii* V1 [32] were grown at 28 °C. *A. salmonicida* subsp. *salmonicida* ATCC 33658^T was grown at 24 °C. *E. coli* K-12 substr. BW25113, *E. coli* NR17793 [31], *Shewanella oneidensis* MR-1^T, *Pseudomonas aeruginosa* PAO1, *Pseudomonas extremaustralis* DSM 25547, *Pseudomonas protegens* Pf-5, *Pseudomonas putida* KT2440, and *Pseudomonas syringae* pv. *syringae* B728a were grown at 28 °C. All strains were grown in lysogeny broth (LB) medium except for *S. oneidensis* that was grown in tryptic soy agar (TSA). After 5 days, incubation cultures were kept at room temperature or 4 °C, and crystal formation was followed using an Olympus Tokyo CK inverted microscope or a stereoscopic microscope Nikon SMZ-745 T. For melanin synthesis inhibition, 1 mM bicyclopiron was added to the growth medium [36].

Characterization of biogenic guanine crystals

Crystals were collected from solid or liquid cultures washing out bacteria and culture residues with water (for SEM) or with solvents with decreasing polarity (water, ethanol and acetone, for XRD, NMR, and ESI-MS experiments), with gentle agitation. Solvent residue was removed by vacuum drying. The crystalline material was then characterized using different techniques (polarized light microscopy, SEM, UV-vis, FT-IR, ESI-MS & MS/MS and ¹H NMR).

Light micrographs using polarized light microscopy (PLM) were taken with a stereoscopic trinocular microscope Nikon SMZ-745 T that includes a lighting

system Nikon Ni-150. Images were processed using the programs Micrometrics™ SE Premium and ImageJ [39]. SEM images were produced using a Carl Zeiss NTS – SUPRA 40. UV–visible spectra of guanine crystals in acid solution (HCl pH 2) were recorded using a Hewlett-Packard 8453 diode array spectrometer. Elemental analysis was carried out in a Carlo Erba CHNS EA-1108 microanalyzer using atropine as standard. FT-IR spectra were recorded using a Nicolet Avatar 320 FTIR spectrometer with a Spectra Tech cell for KBr pellets. High-resolution electrospray ionization mass spectroscopy (HR ESI–MS) was performed using crystals dissolved in a mixture of methanol: DMSO or methanol: H₂O. Mass spectra were recorded on a Xevo G2S Q-TOF (Waters Corp.) instrument, using an electrospray ionization source and quadrupole-flight time analyzer in methanol: water 80:20 or DMSO as solvent. ¹H-NMR spectra were recorded using a Bruker AM500 equipped with a broadband probe. ¹H shifts are reported relative to DMSO-*d*₆ (δ) 2.50 ppm.

Powder X-ray diffraction (powder XRD)

Data were recorded on a PANalytical Empyrean diffractometer equipped with a 4-kW sealed tube Cu K α X-ray radiation (generator power settings: 60 kV and 100 mA) and a PIXcel^{3D} area detector using parallel beam geometry (1/2–1–8 mm slits, 15 mm incident mask). Samples were packed on a silicon monocrystal sample holder that was then placed on the sample holder attachment. For all pXRD experiments, the data were collected over an angle range 5° to 50° with a scanning speed of 23 s per step with 0.026° step.

Comparative genome analysis

The genomes of *Aeromonas* strains and other *Gammaproteobacteria* used for comparative analysis are shown in Additional file 4: Table S3. Global alignments of the genome of 34mel with those of bacterial strains belonging to the genus *Aeromonas* or *Shewanella* were performed using the Needleman-Wunsch algorithm (using the BLOSUM50 scoring matrix and a maximum gap open penalty of 10), which is included in the Bioinformatics Toolbox of Matlab [40]. Phylogenomic tree of *Aeromonas* species was constructed using the tools included in the Type Strain Genome server (TYGS), with FastME 2.1.6.1 [41] from GBDP distances calculated from genome sequences. The branch lengths are scaled in terms of GBDP distance formula d_5 .

Supplementary Information

The online version contains supplementary material available at <https://doi.org/10.1186/s12915-023-01572-8>.

Additional file 1: Figure S1. Crystalline aggregates in colonies from a month-old plate of *A. salmonicida* subsp. *pectinolytica* 34mel. **Figure S2.** Size distribution of the base of the prismatic crystals formed by 34mel grown in different conditions and by *A. media*.

Additional file 2: Figure S3. ESI–MS experiment for guanine produced by 34mel. **Figure S4.** ESI–MS and MS/MS experiments for commercial guanine. **Figure S5.** ¹H-NMR characterization of 34mel crystals. **Figure S6.** UV–vis spectra for commercial and 34mel guanine in acid solution. **Additional data 1.** Elemental analysis of crystals purified from 34mel.

Additional file 3: Additional methods 1. Methods used for the synthesis of the guanine crystalline phases from commercial guanine. **Figure S7.** X-ray diffraction studies of different crystal forms of guanine. **Figure S8.** Crystalline material obtained as result of crystallization experiments of commercial guanine with or without the addition of homogentisate melanin synthesized by 34mel at different pH conditions. **Figure S9.** Powder X-ray diffraction experiments of the crystalline material obtained under different crystallization conditions. **Additional methods 2.** Single crystal X-ray diffraction (XRD) of guaninium chloride dihydrate-melanin. **Figure S10.** Structure of guaninium chloride dihydrate crystallized in presence of melanin produced by the 34mel determined by single crystal X-ray diffraction. **Table S1.** Crystal data and structure refinement for guaninium chloride dihydrate crystallized in presence of melanin produced by 34mel. **Table S2.** Comparative analysis of different guaninium chloride dihydrate single crystal X-ray diffraction data.

Additional file 4: Table S3. Bacteria used for genome analysis.

Acknowledgements

We would like to acknowledge the following: Roberto Servant and Laura Levin for encouraging MEP during the first steps of this research; Alejandro Perretta, Cynthia Sequeiros, and Jorge Trelles who kindly provided us with some *Aeromonas* strains; and Roel Schaaper who generously sent us *E. coli* mutant strains.

Authors' contributions

MEP made the original discovery. MEP, NIL, and MJP conceived the project and performed the microbiological experiments and genomic analysis. MEP, NIL, MJP, FDS, and FM carried out the crystal collection and SEM analysis. FDS and FM performed the chemical characterization experiments and spectroscopic and XRD data analyses. EEP conducted the bioinformatics analyses and genomic comparisons. All authors read and approved the final manuscript.

Funding

This work was supported by grants UBA (20020170100310BA, 20020170100433BA) and ANPCYT (PICT 2016–621) for the purchase of drugs and materials. FDS, NIL, and MJP are staff members of Universidad de Buenos Aires (UBA) and CONICET. FM acknowledges UBA for his scholarships.

Availability of data and materials

The datasets supporting the conclusions of this article are included within the article and its additional files.

Crystallographic data for guaninium chloride dihydrate–melanin have been deposited into the Cambridge Structural Database under the deposition number CCDC 2156488 [42]. These data can be obtained free of charge from The Cambridge Crystallographic Data Centre via www.ccdc.cam.ac.uk/structures.

Declarations

Ethics approval and consent to participate

Not applicable.

Consent for publication

Not applicable.

Competing interests

The authors declare that they have no competing interests.

Received: 4 January 2023 Accepted: 17 March 2023

Published online: 03 April 2023

References

- Wagner A, Ezersky V, Maria R, Upcher A, Lemcoff T, Afalo ED, et al. The non-classical crystallization mechanism of a composite biogenic guanine crystal. *Adv Mater*. 2022;34(31):2202242.
- Gur D, Palmer BA, Weiner S, Addadi L. Light manipulation by guanine crystals in organisms: biogenic scatterers, mirrors, multilayer reflectors and photonic crystals. *Adv Funct Mater*. 2017;27(6):1603514.
- Mojzeš P, Gao L, Ismagulova T, Pilátová J, Moudříková Š, Gorelova O, et al. Guanine, a high-capacity and rapid-turnover nitrogen reserve in microalgal cells. *PNAS*. 2020;117(51):32722–30.
- Aizen R, Tao K, Rencus-Lazar S, Gazit E. Functional metabolite assemblies - a review. *J Nanopart Res*. 2018;20:125.
- Anderson JF. The excreta of spiders. *Comp Biochem Physiol*. 1966;17:973–82.
- Linton S, Wilde JE, Greenaway P. Excretory and storage purines in the anomuran land crab *Birgus latro*; guanine and uric acid. *J Crustac Biol*. 2005;25(1):100–4.
- Creutz CE, Mohanty S, Defalco T, Kretsinger RH. Purine composition of the crystalline cytoplasmic inclusions of *Paramecium tetraurelia*. *Protist*. 2002;153(1):39–45.
- Moudříková Š, Nedbal L, Solovchenko A, Mojzeš P. Raman microscopy shows that nitrogen-rich cellular inclusions in microalgae are microcrystalline guanine. *Algal Res*. 2017;23:216–22.
- DeSa R, Hastings JW. The characterization of scintillons. Bioluminescent particles from the marine dinoflagellate, *Gonyaulax polyedra*. *J Gen Physiol*. 1968;51(1):105–22.
- Guille K, Clegg W. Anhydrous guanine: a synchrotron study. *Acta Cryst*. 2006;C62:o515–7.
- Hirsch A, Gur D, Polishchuk I, Levy D, Pokroy B, Cruz-Cabeza AJ, et al. "Guanigma": the revised structure of biogenic anhydrous guanine. *Chem Mater*. 2015;27(24):8289–97.
- Thewalt U, Bugg CE, Marsh RE. The crystal structure of guanine monohydrate. *Acta Cryst*. 1971;B27:2358–63.
- Gur D, Pierantoni M, Eloom Dov N, Hirsch A, Feldman Y, Weiner S, et al. Guanine crystallization in aqueous solutions enables control over crystal size and polymorphism. *Cryst Growth Des*. 2016;16(9):4975–80.
- Pavan ME, Pavan EE, López NI, Levin L, Pettinari MJ. Living in an extremely polluted environment: clues from the genome of melanin-producing *Aeromonas salmonicida* subsp. *pectinolytica* 34me^T. *Appl Environ Microbiol*. 2015;81(15):5235–48.
- Evans JS. Composite materials design: biomineralization proteins and the guided assembly and organization of biomineral nanoparticles. *Materials*. 2019;12(4):581.
- Gur D, Nicolas JD, Brumfeld V, Bar-Elli O, Oron D, Levkowitz G. The dual functional reflecting iris of the zebrafish. *Adv Sci (Weinh)*. 2018;5(8):1800338.
- Levy-Lior A, Pokroy B, Levavi-Sivan B, Leiserowitz L, Weiner S, Addadi L. Biogenic guanine crystals from the skin of fish may be designed to enhance light reflectance. *Cryst Growth Des*. 2008;8(2):507–12.
- Palmer BA, Taylor GJ, Brumfeld V, Gur D, Shemesh M, Elad N, et al. The image-forming mirror in the eye of the scallop. *Science*. 2017;358(6367):1172–5.
- Pinsk N, Wagner A, Cohen L, Smalley CJ, Hughes CE, Zhang G, et al. Biogenic guanine crystals are solid solutions of guanine and other purine metabolites. *J Am Chem Soc*. 2022;144(11):5180–9.
- Jantschke A, Pinkas I, Hirsch A, Elad N, Schertel A, Addadi L, et al. Anhydrous β -guanine crystals in a marine dinoflagellate: structure and suggested function. *J Struct Biol*. 2019;207(1):12–20.
- Rice JM, Dudek GO. Mass spectra of nucleic acid derivatives. II. Guanine, adenine, and related compounds. *J Am Chem Soc*. 1967;89(11):2719–25.
- Levy-Lior A, Shimoni E, Schwartz O, Gavish-Regev E, Oron D, Oxford G, et al. Guanine-based biogenic photonic-crystal arrays in fish and spiders. *Adv Funct Mater*. 2010;20(2):320–9.
- Djurdjević I, Krefl ME, Sušnik BS. Comparison of pigment cell ultrastructure and organisation in the dermis of marble trout and brown trout, and first description of erythrofore ultrastructure in salmonids. *J Anat*. 2015;227(5):583–95.
- Greene SE, Komeili A. Biogenesis and subcellular organization of the magnetosome organelles of magnetotactic bacteria. *Curr Opin Cell Biol*. 2012;24(4):490–5.
- Nair K, Al-Thani R, Al-Thani D, Al-Yafei F, Ahmed T, Jaoua S. Diversity of *Bacillus thuringiensis* strains from Qatar as shown by crystal morphology, δ -endotoxins and cry gene content. *Front Microbiol*. 2018;9:708.
- Higdon CW, Mitra RD, Johnson SL. Gene expression analysis of zebrafish melanocytes, iridophores, and retinal pigmented epithelium reveals indicators of biological function and developmental origin. *PLoS ONE*. 2013;8:e67801.
- Farkas WR, Stanawitz T, Schneider M. Saturnine gout: Lead-induced formation of guanine crystals. *Science*. 1978;199(4330):786–7.
- Waite ME, Walker G. Guanine in *Balanus balanoides* (L.) and *Balanus crenatus* Bruguiere. *J Exp Mar Biol Ecol*. 1984;77(1–2):11–21.
- Farris JS. Estimating phylogenetic trees from distance matrices. *Am Nat*. 1972;106(951):645–67.
- Seffernick JL, Dodge AG, Sadowsky MJ, Bumpus JA, Wackett LP. Bacterial ammeline metabolism via guanine deaminase. *J Bacteriol*. 2010;192(4):1106–12.
- Itsko M, Schaaper RM. Transcriptome analysis of *Escherichia coli* during dGTP starvation. *J Bacteriol*. 2016;198(11):1631–44.
- Perretta A, Antúnez K, Zunino P. Phenotypic, molecular and pathological characterization of motile aeromonads isolated from diseased fishes cultured in Uruguay. *J Fish Dis*. 2018;41(10):1559–69.
- Pilátová J, Pánek T, Oborník M, Čepička I, Mojzeš P. Revisiting biocrystallization: purine crystalline inclusions are widespread in eukaryotes. *ISME J*. 2022;16:2290–4.
- Lewis AC, Rankin KJ, Pask AJ, Stuart-Fox D. Stress-induced changes in color expression mediated by iridophores in a polymorphic lizard. *Ecol Evol*. 2017;7(20):8262–72.
- Hirata M, Nakamura K, Kanemaru T, Shibata Y, Kondo S. Pigment cell organization in the hypodermis of zebrafish. *Dev Dyn*. 2003;227(4):497–503.
- Pavan ME, Venero ES, Egoburo DE, Pavan EE, López NI, Pettinari MJ. Glycerol inhibition of melanin biosynthesis in the environmental *Aeromonas salmonicida* 34me^T. *Appl Microbiol Biotechnol*. 2019;103:1865–76.
- Wagner A, Wen Q, Pinsk N, Palmer BA. Functional molecular crystals in biology. *Isr J Chem*. 2021;61(9–10):668–78.
- Soldo AT, Godoy GA, Larin F. Purine-excretory nature of refractile bodies in the marine ciliate *Parauronema acutum*. *J Protozool*. 1978;25(3):416–8.
- Schneider CA, Rasband WS, Eliceiri KW. NIH Image to ImageJ: 25 years of image analysis. *Nat Methods*. 2012;9(7):671–5.
- Henson R, Cetto L. The MATLAB bioinformatics toolbox. In *Encyclopedia of Genetics, Genomics, Proteomics and Bioinformatics*. Edited by Jorde L, Little P, Dunn M, Subramaniam S. New Jersey: Wiley; 2005:105.
- Lefort V, Desper R, Gascuel O. FastME 2.0: a comprehensive, accurate, and fast distance-based phylogeny inference program. *Mol Biol Evol*. 2015;32(10):2798–800.
- Crystallographic data for guaninium chloride dihydrate – melanin. Cambridge Structural Database (CCDC). 2022 <https://www.ccdc.cam.ac.uk/structures/Search?Ccdcid=2156488>.

Publisher's Note

Springer Nature remains neutral with regard to jurisdictional claims in published maps and institutional affiliations.